

## Endothelial tetraspanin microdomains regulate leukocyte firm adhesion during extravasation

Olga Barreiro, María Yáñez-Mó, Mónica Sala-Valdés, María Dolores Gutiérrez-López, Susana Ovalle, Adrian Higginbottom, Peter N. Monk, Carlos Cabañas, and Francisco Sánchez-Madrid

**Tetraspanins associate with several transmembrane proteins forming microdomains involved in intercellular adhesion and migration. Here, we show that endothelial tetraspanins relocate to the contact site with transmigrating leukocytes and associate laterally with both intercellular adhesion molecule-1 (ICAM-1) and vascular cell adhesion molecule-1 (VCAM-1). Alteration of endothelial tetraspanin**

**microdomains by CD9–large extracellular loop (LEL)–glutathione S–transferase (GST) peptides or CD9/CD151 siRNA oligonucleotides interfered with ICAM-1 and VCAM-1 function, preventing lymphocyte transendothelial migration and increasing lymphocyte detachment under shear flow. Heterotypic intercellular adhesion mediated by VCAM-1 or ICAM-1 was augmented when expressed exogenously in**

**the appropriate tetraspanin environment. Therefore, tetraspanin microdomains have a crucial role in the proper adhesive function of ICAM-1 and VCAM-1 during leukocyte adhesion and transendothelial migration. (Blood. 2005;105:2852-2861)**

© 2005 by The American Society of Hematology

### Introduction

Plasma membrane contains small organized microdomains (lipid rafts) in which restricted repertoires of proteins are arranged together.<sup>1,2</sup> In resting cells, lipid rafts are estimated to be around 100 nm in diameter, including a few dozen proteins, and are distributed randomly on the cell surface, covering up to 50% of the plasma membrane. Upon cell activation, raft domains coalesce, recruiting and excluding different receptors, and allowing the proper organization of signaling complexes for efficient signal transduction.<sup>1,2</sup>

Tetraspanins comprise a large number of small palmitoylated polypeptides that span the plasma membrane 4 times,<sup>3-6</sup> and form microdomains that contain a restricted repertoire of proteins. Biochemically, they share some properties with lipid rafts, but tetraspanin microdomains are based on protein-protein interactions.<sup>7-10</sup> Tetraspanins have a highly conserved structure with a short and a large extracellular loop (LEL) where 2 or 3 disulfide bonds can be formed.<sup>11</sup> This large loop interacts noncovalently with other tetraspanins and transmembrane proteins, including integrins and adhesion receptors of the immunoglobulin (Ig) superfamily. Although all mammalian cells express different tetraspanins, genetic approaches have been elusive and their function has not yet been fully elucidated. However, their role in antigen presentation and sperm-egg binding has been recently underscored.<sup>12-20</sup>

The association of certain plasma membrane proteins to the cortical actin cytoskeleton is critical for their proper localization and function. Thus, the concentration of selectins and their ligands

on the tip of microvilli<sup>21,22</sup> both at the leukocyte and the apical surface of endothelial cells favors their interaction during the rolling phase of leukocyte extravasation. Likewise, vascular cell adhesion molecule-1 (VCAM-1) and intercellular adhesion molecule-1 (ICAM-1), which are relevant in the subsequent leukocyte firm adhesion step, are also displayed anchored to actin through ezrin-radixin-moesin proteins (ERMs)<sup>23,24</sup> at the apical surface on endothelial cells. Upon leukocyte firm adhesion, the engagement of VCAM-1 and ICAM-1 triggers the reorganization of the endothelial cortical actin cytoskeleton, building up a 3-dimensional docking structure that prevents the detachment of leukocytes by shear stress.<sup>22,23</sup> Here, we show that ICAM-1 and VCAM-1 are included in tetraspanin microdomains that regulate their membrane expression and the efficient adhesive function necessary for proper leukocyte transendothelial migration under flow conditions.

### Materials and methods

#### Cells and cell cultures

Human umbilical vein endothelial cells (HUVECs) were obtained and cultured as previously described.<sup>25</sup> Cells were used up to the third passage in all assays. To activate HUVECs, tumor necrosis factor- $\alpha$  (TNF- $\alpha$ ; 20 ng/mL)(R&D Systems, Minneapolis, MN) was added to the culture media 20 hours before the assays were performed. T lymphoblasts were derived

From the Servicio de Inmunología, Hospital de la Princesa, Universidad Autónoma de Madrid, Spain; Instituto de Farmacología y Toxicología, Consejo Superior de Investigaciones Científicas–Universidad Complutense de Madrid (CSIC-UCM), Facultad de Medicina, Universidad Complutense, Madrid, Spain; and Department of Academic Neurology, The Medical School, University of Sheffield, United Kingdom.

Submitted September 17, 2004; accepted November 26, 2004. Prepublished online as *Blood* First Edition Paper, December 9, 2004; DOI 10.1182/blood-2004-09-3606.

Supported by grants BMC-2002 00563 from the Ministerio de Ciencia y Tecnología, Ayuda a la Investigación Básica Juan March 2002, and FIPSE 36289/02 (F.S.-M.), SAF2001-2807 from the Ministerio de Ciencia y Tecnología (C.C.), British Heart Foundation PG/98163 (P.N.M.), and fellowships from Red

Cardiovascular from FIS and EU grant LSHG-CT-2003-502935 (O.B.) and from FIS (M.Y.-M.).

O.B. and M.Y.-M. contributed equally to this manuscript.

The online version of the article contains a data supplement.

**Reprints:** Francisco Sánchez-Madrid, Servicio de Inmunología, Hospital de la Princesa, Universidad Autónoma de Madrid, C/ Diego de León 62, 28006 Madrid, Spain; e-mail: fsanchez.hlpr@salud.madrid.org.

The publication costs of this article were defrayed in part by page charge payment. Therefore, and solely to indicate this fact, this article is hereby marked "advertisement" in accordance with 18 U.S.C. section 1734.

© 2005 by The American Society of Hematology

from freshly isolated human peripheral blood lymphocytes (PBLs) by activation with phytohemagglutinin-L (PHA-L) (1  $\mu\text{g}/\text{mL}$ ; Sigma, St Louis, MO) for 24 hours followed by culture for 7 to 14 days in the presence of recombinant human (rh) interleukin-2 (IL-2; 50 U/mL) obtained from M. Gately (Hoffmann-LaRoche, Nutley, NJ) was provided by the National Institutes of Health AIDS Research and Reference Reagent program, Division of AIDS. Human PBLs, monocytes, neutrophils, and K562 erythroleukemic cells stably transfected with the  $\alpha 4$  or lymphocyte function-associated antigen-1 (LFA-1) integrins were obtained and cultured as described.<sup>23</sup> Adhesion of K562 LFA-1 transfectants to Colo320 colocal carcinoma cell line was performed in the presence of 1mM  $\text{Mn}^{2+}$  to induce integrin activation. Colo320-CD9 and chimeric Colo320-CD9  $\times$  82 and Colo320-CD82CCG9 are stably transfected clones derived from those previously described.<sup>26</sup> Approval was obtained from the Hospital Universitario de la Princesa institutional review board for these studies. Informed consent was provided according to the Declaration of Helsinki.

### Antibodies and recombinant DNA constructs and proteins

Monoclonal antibodies (mAbs) anti-CD151 (LIA1/1), anti- $\beta 1$  integrin (TS2/16), anti-vascular endothelial (VE)-cadherin (TEA1/31), anti-E-selectin (TEA2/1), anti-CD44 (HP2/9), anti-CD63 (Tea3/18), and anti-CD9 (VJ1/20) have been previously described.<sup>25,27-29</sup> The 4B9 and P8B1 (anti-VCAM-1), Hu5/3 (anti-ICAM-1), 10B1 (anti-CD9), TS82 (anti-CD82), 8C3 (anti-CD151), and I.33.22 (anti-CD81) mAbs were kindly provided by R. Lobb (Biogen, Cambridge, MA), E. A. Wayner (Fred Hutchinson Cancer Research Center, Seattle, WA), F. W. Luscinskas (Brigham and Women's Hospital and Harvard Medical School, Boston, MA), E. Rubinstein (INSERM U268, Villejuif, France), K. Sekiguchi (Osaka University, Japan), and R. Vilella (Hospital Clinic, Barcelona, Spain), respectively. The IgG1, $\kappa$  mAb from the P3  $\times$  63 myeloma cell line was used as negative control. Anti-GST goat polyclonal Ab was purchased from Amersham Biosciences (Uppsala, Sweden), and anti-vimentin mAb was purchased from Sigma.

ICAM-1, VCAM-1, CD9, and CD151-green fluorescent protein (GFP) tagged proteins have been described.<sup>23,30</sup> The LEL-GST peptides of wild-type human CD9 or the mutated forms in the Cys residues have also been described.<sup>31</sup> The corresponding CD151-LEL-GST peptide presented a low rate of proper folding in solution which precluded its use in functional studies.

### Flow cytometry analysis, immunofluorescence, and confocal microscopy

For flow cytometry analysis and immunofluorescence experiments, cells were treated as previously described.<sup>25</sup> Paraformaldehyde solution (4%) was used as a fixative in all samples. Alexa Fluor 488 goat anti-mouse IgG conjugate and rhodamine red-X-Affinipure streptavidin were used as fluorescent reagents (Molecular Probes, Eugene, OR). A series of optical sections were obtained with a Leica TCS-SP confocal laser scanning unit equipped with Ar and He/Ne laser beams and attached to a Leica DMIRBE inverted epifluorescence microscope (Leica Microsystems, Heidelberg, Germany), using a PL APO 63  $\times$  1.32-0.6 oil immersion objective.

### Time-lapse fluorescence confocal microscopy

Transiently transfected HUVECs were generated by electroporation at 200 V and 975  $\mu\text{F}$  using a Gene Pulser (Bio-Rad Labs, Hercules, CA), and adding 20  $\mu\text{g}$  of each DNA construct. These cells were grown to confluence for 24 to 48 hours on glass-bottom dishes (WillCo Wells, Amsterdam, the Netherlands) precoated with fibronectin (20  $\mu\text{g}/\text{mL}$ ; Sigma). Cells were activated with TNF- $\alpha$  for 20 hours; then, T lymphoblasts resuspended in 500  $\mu\text{L}$  of complete 199 medium (BioWhittaker, Verviers, Belgium) were added. During the observation time, plates were maintained at 37°C in a 5%  $\text{CO}_2$  atmosphere using an incubation system (La-con GB Pe-con GmbH, Erbach, Germany). Confocal series of fluorescence and differential interference contrast (DIC) images, distanced 0.4  $\mu\text{m}$  in the z-axis, were simultaneously obtained at 30-second or 1 minute intervals with a  $\times$  63 oil immersion objective. Images were processed and assembled into movies using Leica Confocal software.

### Coimmunoprecipitation assays

Coimmunoprecipitation experiments were performed as previously described<sup>25</sup> with TNF- $\alpha$ -activated HUVEC lysates obtained in 1% Brij96 (Sigma) in 1 mM  $\text{Ca}^{2+}$  and 1 mM  $\text{Mg}^{2+}$  Tris-buffered saline (TBS) with protease inhibitors.

### Small interference RNA assay

To selectively knock down the expression of endothelial tetraspanins CD9 and CD151, a screening of different target sequences for each protein was performed using siRNA expression cassettes (Ambion, Austin, TX). We found the silencing sequences GAGCATCTTCGAGCAAGAA and CATGTGGCACCGTTTGCCCT for CD9 and CD151, respectively. RNA duplexes corresponding to these target sequences, as well as a negative oligonucleotide that does not pair with any human mRNA, designed by Eurogentec (Seraing, Belgium), were used. Oligos were transfected in HUVECs with oligofectamine (Invitrogen, Carlsbad, CA) following manufacturer's instructions. For CD9 interference, cells were transfected on day 0, further split on day 2, and retransfected on day 3. In parallel, on day 3, cells were transfected only once for CD151 knocking down. Then, cells were trypsinized on day 6 and negatively selected with anti-CD9 or anti-CD151 magnetic coated beads (Dynabeads M450 Goat anti-Mouse IgG; DYNAL Biotech ASA, Oslo, Norway) for 3 to 5 minutes at 4°C under rotation to enrich the tetraspanin low-expressing population. Cells thus selected were counted and seeded onto fibronectin to confluence for the different experiments, since its receptor  $\alpha 5\beta 1$  expression was not altered by tetraspanin knocking down (not shown).

### Paracellular monolayer permeability measurements

HUVEC monolayer paracellular permeability measurements were performed in 0.4- $\mu\text{m}$  pore diameter Transwells (Costar, Corning, NY) with 77 kDa fluorescein isothiocyanate (FITC)-labeled dextran (Sigma) as described.<sup>32</sup>

### Adhesion and transendothelial migration assays

Adhesion of human PBLs to HUVEC monolayers was performed in static conditions for 15 minutes at 37°C and measured as described.<sup>23</sup>

PBL migration through a confluent monolayer of activated HUVECs was assayed in 3- $\mu\text{m}$  pore Transwell cell culture chambers (Costar). HUVECs were grown to confluence on Transwell inserts precoated with 1% fixed gelatin or 20  $\mu\text{g}/\text{mL}$  of fibronectin and activated with TNF- $\alpha$  for 20 hours in the presence or not of 150  $\mu\text{g}/\text{mL}$  of the LEL-GST fusion proteins or after knocking down tetraspanin proteins. Monolayers were washed and freshly isolated PBLs ( $2 \times 10^5$  in 100  $\mu\text{L}/\text{well}$ ) were added to the upper chambers. In the lower well, 600  $\mu\text{L}$  of complete 199 medium, with or without 100 ng/mL of human recombinant stromal cell-derived factor-1 $\alpha$  (SDF-1 $\alpha$ ; R&D Systems, Minneapolis, MN) were poured. Chambers were incubated for 2 to 7 hours at 37°C. Migrated lymphocytes, ranging from 5% to 20%, were recovered from the lower chamber and estimated by flow cytometry.

### Parallel plate flow chamber analysis of endothelial-PBL interactions and detachment experiments

The parallel plate flow chamber used for leukocyte adhesion and detachment under defined laminar flow has been described in detail.<sup>33</sup> PBLs ( $1 \times 10^6/\text{mL}$ ) were drawn across activated confluent monolayers at an estimated wall shear stress of 1.8  $\text{dyn}/\text{cm}^2$  for 10 minutes. Lymphocyte rolling on the endothelium was easily visualized since they traveled more slowly than free-flowing cells. Lymphocytes were considered to be adherent after 20 seconds of stable contact with the monolayer. Transmigrated lymphocytes were determined as those being beneath the endothelial monolayer. Lymphocytes were considered to be detached when they returned to a free-flowing state after having established a transient contact with the endothelium. The number of rolling, adhered, transmigrated, and detached cells was quantified by direct visualization of 6 different fields ( $\times$  20 phase-contrast objective) for 30 seconds starting at 3.5 minutes and

ending at 6.5 minutes. Digitalization was performed with Optimas software (Bioscan).

For detachment experiments, peripheral blood lymphocytes were allowed to adhere for 15 minutes at 37°C to activated HUVEC monolayers, either incubated with LEL-GSTs for 20 hours, or transfected with siRNA oligos. Then, shear stress was applied by pulling assay buffer (Hanks balanced salt solution [HBSS] buffer with 2% fetal calf serum [FCS]) through the flow chamber with a programmable syringe pump, starting at 2 dyn/cm<sup>2</sup> and increasing up to 30 dyn/cm<sup>2</sup> at 1-minute intervals. The number of cells attached after each shear stress interval was quantified in 4 to 8 fields ( $\times 20$  phase-contrast objective). Cell detachment was obtained from the difference in adhered cells after subtracting the percentage of cells that had transmigrated during the assay.

### Heterotypic intercellular binding assays

Colo320 colocal carcinoma cells or different stable transfectants derived from this cell line were transiently transfected with ICAM-1-GFP or VCAM-1-GFP by electroporation in an ElectroSquarePorator ECM 830 (BTX, VWR, San Diego, CA). A total of  $5 \times 10^5$  cells of each condition were mixed with  $2 \times 10^5$  of K562 cells, either untransfected or stably transfected with  $\alpha 4$  or LFA-1 integrins, which had been previously loaded with the CM-TMR (5-(and-6)-((4-chloromethyl)benzoyl)amino)tetramethylrhodamine red fluorescent dye (Molecular Probes). Then, cells were allowed to adhere at room temperature under rotatory conditions for 90 minutes in RPMI medium without supplements. The relative number of heterotypic intercellular binding was estimated by flow cytometry.

## Results

### Tetraspanins are components of the endothelial docking structure for adherent leukocytes by their association with ICAM-1 and VCAM-1

Tetraspanin proteins are low-molecular-weight polypeptides that are able to associate with a variety of transmembrane proteins via their extracellular domain, forming multiproteic domains in the plasma membrane. They have been involved in several cellular functions including intercellular homotypic and heterotypic adhesion;<sup>6</sup> however, genetic approaches directed to tetraspanins did not render clear-cut information on their individual functional roles. HUVECs express several of these proteins (CD9, CD81, CD151, CD63), both at intercellular contacts and intracellular vesicles.<sup>25,34</sup> On the other hand, T lymphoblasts express CD81 and low levels of CD151, whereas the expression of CD9 is heterogeneous, ranging from completely negative to high expressing cells, and the relative amount of each population varies in different human donors. Upon T lymphoblast adhesion onto activated HUVEC monolayers, endothelial tetraspanins redistributed, together with ICAM-1 and VCAM-1, to the docking structure that emerges from the apical surface to firmly attach the transmigrating cell<sup>22,23</sup> (Figure 1A-B, and data not shown). Tetraspanin redistribution was also observed under flow conditions around adherent peripheral blood lymphocytes, neutrophils, or monocytes (Figure 1C for CD9, and data not shown).

To determine the subcellular localization of endothelial tetraspanins during the whole transendothelial migration process, T lymphoblasts were allowed to transmigrate across TNF- $\alpha$ -activated HUVEC monolayers. CD9 clustering was evident in those lymphocyte-endothelial interactions occurring at the apical surface of the monolayer (Figure 1D, white arrows). In contrast, almost no redistribution of CD9 could be observed at the ventral surface of endothelial cells in contact with transmigrated lymphoblasts (Figure 1D, gray arrows). On the other hand, CD151 relocalization around lymphoblasts was

clearly detected at both the apical and basal surface of the endothelial cell (Figure 1D; white and gray arrows, respectively), paralleling the behavior of ICAM-1. Similarly to that observed with the endogenous protein stainings, CD9-GFP was more clearly relocalized to the contact site with T lymphoblasts at the endothelial apical surface, although some clustering occurred around transmigrated lymphoblasts locomoting underneath the endothelium (Supplemental Video S1; see the Supplemental Video link at the top of the online article on the *Blood* website). On the other hand, CD151-GFP was strongly concentrated at the contact with lymphoblasts throughout all the transmigration process (Video S2). These data point to the existence of different tetraspanin microdomains at the apical and ventral endothelial surfaces and suggest a complex dynamic regulation of these membrane domains.

Tetraspanin interactions are biochemically detected by extraction with Brij 96/97 detergents. Although HUVEC tetraspanins were mostly associated with EWI-F and  $\beta 1$  integrins (Yáñez-Mó et al<sup>25</sup> and data not shown), CD9 and CD151 were also able to pull down ICAM-1 and VCAM-1 (Figure 1E). Conversely, ICAM-1 mAbs were also able to coprecipitate CD9, whereas VCAM-1 mainly coprecipitated CD151. No detectable signal for ICAM-1 was observed in  $\beta 1$  immunoprecipitates (not shown), suggesting that tetraspanin-integrin complexes are different to tetraspanin/ICAM-1/VCAM-1 complexes. Coprecipitation of CD9 and CD151 with ICAM-1 and VCAM-1 could also be faintly detected upon extraction with 1% digitonin (not shown), conditions in which most interactions among tetraspanins are lost and direct tetraspanin-partner associations are observed.<sup>35</sup> These results indicate that ICAM-1 and VCAM-1 are included into tetraspanin microdomains.

### Tetraspanin microdomains are critical for a proper expression and function of ICAM-1 and VCAM-1

In order to gain insights into the relevance of the inclusion of ICAM-1 and VCAM-1 into tetraspanin microdomains at endothelial cells, we used an siRNA approach against tetraspanins CD9 and CD151 in primary human endothelial cells. Endothelial tetraspanin CD9 and CD151 expression was considerably knocked down with specific siRNA oligos. In no case was the expression completely abolished, but a significant reduction (40%-70%) was attained (Figure 2A and B; flow cytometry analysis depicted in logarithmic scale and mean fluorescence quantified in Figure 2C). In immunofluorescence analyses a clear reduction of tetraspanin staining could be observed, with some cells showing expression levels even below the detection threshold (Figure 2D). A compensation effect on the expression of other tetraspanins was observed (Figure 2B-D).

HUVECs thus treated were viable and clearly responded to TNF- $\alpha$ , increasing ICAM-1, VCAM-1, and E-selectin expression over resting levels (ICAM-1 expression increased 10- to 30-fold upon TNF- $\alpha$  treatment, whereas VCAM-1 and E-selectin were undetectable in resting cells; Figure 3A, dotted line). The siRNA transfection procedure slightly affected the inducible expression of these adhesion receptors when compared with untransfected cells, as determined with a negative oligonucleotide control that does not pair with any human mRNA (not shown). In CD9 or CD151 tetraspanin-interfered cells, a selective reduction in the expression of ICAM-1 and VCAM-1, but not that of E-selectin or CD44 was observed (Figure 3A, thick versus thin line). This reduction was of 60%



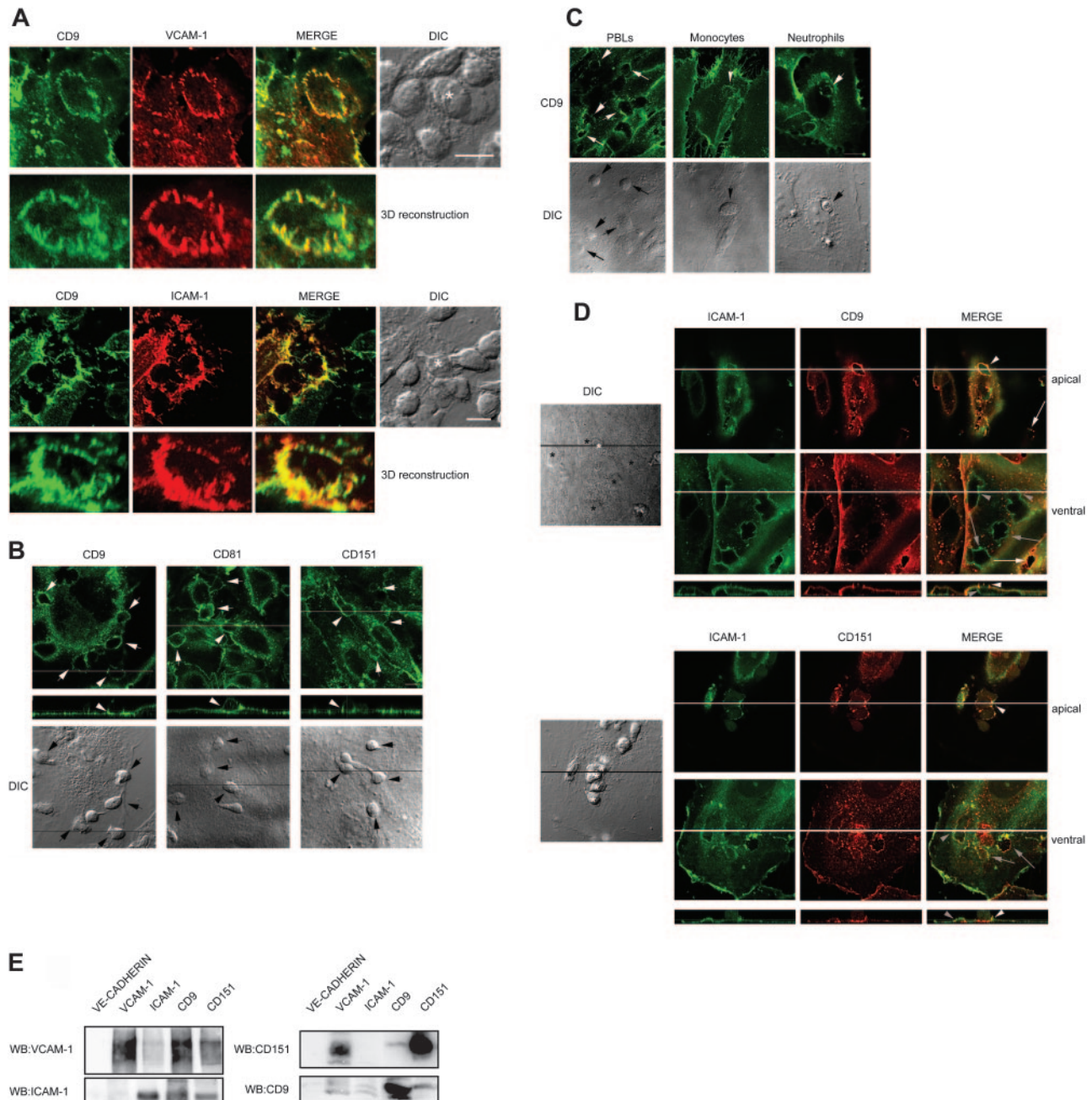


**Figure 1. Endothelial tetraspanin proteins relocalize to the contact site with adherent leukocytes and associate with ICAM-1 and VCAM-1.** (A) T lymphoblasts were adhered to TNF- $\alpha$ -activated HUVEC monolayers, fixed, and double-stained for CD9 and VCAM-1 or ICAM-1. Maximum projections of the relevant sections from the confocal stacks and the merge of both channels are shown. Asterisks in differential interference contrast (DIC) images highlight the T lymphoblasts around which the docking structures shown in the 3-dimensional (3D) reconstructions are formed. Scale bars equal 10  $\mu$ m. (B) T lymphoblasts were adhered to TNF- $\alpha$ -activated HUVEC monolayers, fixed, and stained with antitetraspanin mAbs VJ1/20 (anti-CD9), I.33.2.2 (anti-CD81), and LIA1/1 (anti-CD151). Confocal stacks were obtained and representative apical horizontal and vertical sections together with the corresponding DIC images are shown. Arrows point to the positions of the adhered lymphoblasts. Scale bar equals 10  $\mu$ m. (C) Human PBLs, neutrophils, or monocytes were perfused at physiologic flow rate (1.8 dyn/cm<sup>2</sup>), fixed, and stained with anti-CD9 VJ1/20 mAb. Confocal stacks were obtained and maximum projections of the whole series or a representative section together with the corresponding DIC images are shown. Arrows point to the position of the adhered leukocytes. Scale bar equals 20  $\mu$ m. (D) Analysis of the localization of endogenous endothelial CD9 or CD151, compared with ICAM-1, at apical and ventral contact sites with transmigrating lymphocytes. Human T lymphoblasts were allowed to transmigrate through TNF- $\alpha$ -activated HUVECs, fixed, and double-stained with antitetraspanin mAbs and biotin-conjugated anti-ICAM-1. Confocal stacks were obtained and representative sections at apical or ventral positions of the same field together with the corresponding DIC image are displayed. White arrows and asterisks mark apically adhered lymphocytes, and gray arrows and black asterisks mark those lymphocytes that have transmigrated. Arrowheads and lines point to the position of the adhered or transmigrated lymphoblast shown in the vertical sections. Scale bar equals 10  $\mu$ m. (E) ICAM-1 and VCAM-1 are associated with tetraspanins in TNF- $\alpha$ -activated HUVECs. Cell lysates were obtained in 1% Brij96 and immunoprecipitated with the different mAbs specific for endothelial adhesion molecules or tetraspanins. After washing, immunoprecipitates were resolved in sodium dodecyl sulfate–polyacrylamide gel electrophoresis (SDS-PAGE) gels and revealed by Western blot for VCAM-1 (P8B1), ICAM-1 (HU5/3), CD151 (8C3) or CD9 (VJ1/20).

for ICAM-1 and 80% for VCAM-1 when compared with their expression in negative oligonucleotide-transfected cells to exclude any off-target effect caused by siRNA transfection (Figure 3B). These data further emphasize the importance of tetraspanin

microdomains in ICAM-1 and VCAM-1 expression and suggest that their association with tetraspanins occurs early in the biosynthetic processing of these Ig adhesion molecules, or that it is necessary for their proper membrane insertion or retention.

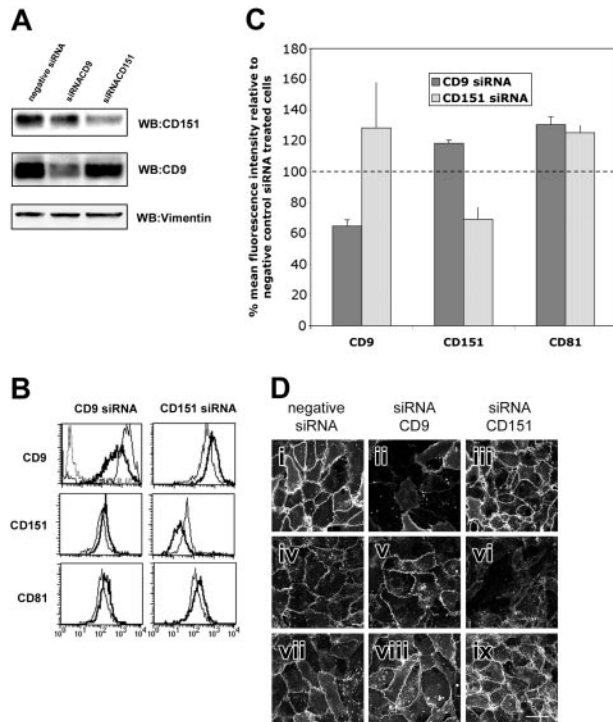


**Figure 2.** siRNA knocking down of tetraspanins CD9 and CD151 in HUVECs. (A) Analysis by Western blot of the expression of tetraspanins CD9 and CD151 in total-cell lysates of siRNA-transfected cells. Loading control for vimentin is also shown. Densitometric analysis of the experiment shown gave a reduction in the total protein amount of 70% for CD151 and 40% for CD9 expression. (B) Flow cytometry analysis of the expression of tetraspanins (anti-CD9 VJ1/20, anti-CD151 LIA1/1, anti-CD81 1.33.2.2) in tetraspanin siRNA-treated HUVECs. Negative siRNA-treated cells are shown in thin lines. Thick lines correspond to the expression in tetraspanin siRNA-transfected cells. Negative control PX63 is shown in dotted lines. The histograms are depicted in a logarithmic scale. (C) Quantitative analysis of the mean fluorescence intensity of CD9, CD151, and CD81 in tetraspanin siRNA-transfected cells. Data represent the mean of 2 independent experiments  $\pm$ SD as the percentage of the expression referred to that of negative control siRNA-transfected cells. (D) Immunofluorescence analysis of CD9 (i-iii), CD151 (iv-vi), and CD81 expression (vi-ix) and localization in HUVECs transfected with siRNA specific for endothelial tetraspanins CD9 and CD151 as well as the negative oligonucleotide. Images were acquired by confocal microscopy using the same photomultiplier parameters in control and tetraspanin-interfered cells. Maximum projection of the whole confocal image stack is shown. Scale bar equals 40  $\mu$ m.

Although ICAM-1 and VCAM-1 expression was lower in tetraspanin-interfered HUVECs, no difference was observed in peripheral blood lymphocyte (PBL) adhesion to interfered monolayers when performed under static conditions (Figure 3C). However, when HUVECs treated with siRNA oligos were seeded onto Transwell insets to perform chemotactic transmigration assays with human PBLs, a strong inhibition of lymphocyte transmigration was observed with both CD9 and CD151 siRNA-treated endothelial monolayers as compared with cells transfected with the negative control oligonucleotide (Figure 3D).

Given that ICAM-1 and VCAM-1 are components of a docking structure whose relevance in leukocyte firm adhesion was unveiled under flow conditions,<sup>23</sup> we assessed the role of tetraspanin microdomains on the strength of lymphocyte adhesion to endothelial cells by measuring their resistance to detachment under increasing shear stress. After 15 minutes, PBL adhesion to TNF- $\alpha$ -activated HUVECs was highly resistant to laminar flow, and most cells still remained attached at 10 dyn/cm<sup>2</sup> (5-fold more than physiologic shear stress) in control HUVEC monolayers (Figure 3E). In contrast, a great proportion of the PBLs adhered on tetraspanin-interfered monolayers started to detach even at low flow rates (Figure 3E).

When extravasation assays using tetraspanin-interfered endothelium were performed under physiologic flow conditions, a significant reduction in the number of adherent lymphocytes was also observed (Figure 3F). Furthermore, a tendency to decrease was consistently observed in rolling and transmigration. All these differences might be related to the lower ICAM-1 and VCAM-1 expression levels in tetraspanin-interfered cells or, additionally, the insertion of these molecules into tetraspanin-based microdomains might be critical for their proper function under shear stress conditions.

#### Tetraspanin-soluble peptides interfere with ICAM-1 and VCAM-1 function without affecting their surface expression

Tetraspanin associations with other transmembrane proteins occur through their LELs.<sup>11</sup> We thus generated soluble GST-LEL peptides from human CD9 (Figure 4A) and point mutants to Ala of any of the 4 Cys residues in the LEL of CD9, which show altered disulphide bond formation and tertiary conformation (Figure 4A). Although some degree of degradation of the soluble peptide occurs, a great proportion of the material eluted from the columns was reactive with CD9 mAb in Western blot under nonreducing conditions (Figure 4A). Incubation of HUVECs with GST-LEL peptides affected neither the expression levels of ICAM-1 and VCAM-1 induced by TNF- $\alpha$  (Figure 4B), nor cell viability (Figure 4C) or monolayer permeability (Figure 4D). The soluble peptides were added to the preparations at the time of addition of TNF- $\alpha$  so that they were accessible at the earliest time of inducible expression of both adhesion receptors. Thus, these peptides allowed us to interfere with tetraspanin-based microdomains without altering the expression levels of ICAM-1 or VCAM-1 induced by TNF- $\alpha$ . Incubation of HUVECs with CD9-LEL-GST, but not the mutated forms, significantly inhibited transendothelial migration of lymphocytes (Figure 5A), whereas they did not affect lymphocyte chemotaxis across nude Transwells (data not shown). When adhered PBLs were subjected to increasing shear stress, a higher PBL detachment rate was also observed upon treatment of HUVECs with CD9-LEL-GST (Figure 5B), but not with the point mutants. In these experiments the number of lymphocytes that transmigrated along the assay was also significantly reduced in those preparations treated with CD9-GST (not shown). All these data demonstrate that tetraspanin microdomains are important not only for proper ICAM-1 and VCAM-1 expression on the plasma membrane but also for their efficient adhesive function under flow conditions.

#### Enhanced ICAM-1 and VCAM-1 adhesive function requires an appropriate tetraspanin environment

To address the relevance of the repertoire of tetraspanin microdomains in the presentation of ICAM-1 and VCAM-1 adhesion molecules, we used Colo320 colocal carcinoma cells and a CD9 stable transfectant in this cell line. Colo320 cells express similar levels of CD151, CD81, CD63, and CD82 on the plasma membrane than endothelial cells, without expression of CD9, ICAM-1, or VCAM-1 (Figure 6A). A down-regulation of CD81 and CD63 was also observed upon stable transfection of these cells with CD9 (Figure 6A). Then, Colo320 and Colo320-CD9 were transiently transfected with VCAM-1 or ICAM-1-GFP to allow their heterotypic binding to  $\alpha$ 4- or LFA-1-transfected K562 cells. The levels of ICAM-1 and VCAM-1 expression attained by transient transfection varied among the different cell lines and experiments, but only cells with comparable high expression were analyzed in functional assays.

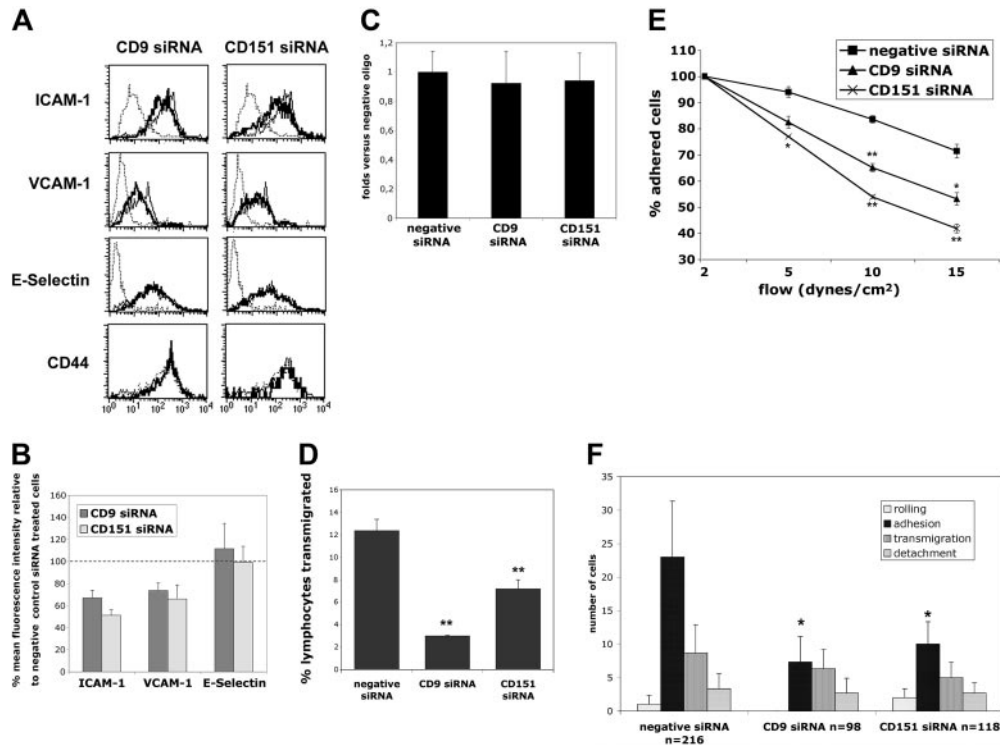


**Figure 3. Tetraspanin interference affects ICAM-1 and VCAM-1 expression and function.** (A) Flow cytometry analysis of the expression of adhesion molecules ICAM-1 (HU5/3), VCAM-1 (P8B1), E-Selectin (TEA2/1), and CD44 (HP2/9) in tetraspanin siRNA-treated HUVECs. TNF- $\alpha$ -activated negative siRNA-treated cells are shown in thin lines. Thick lines correspond to the expression in TNF- $\alpha$ -activated tetraspanin siRNA-transfected cells. Expression of the different adhesion molecules in resting cells is shown in dotted lines. The histograms are depicted in a logarithmic scale. (B) Quantitative analysis of the mean fluorescence intensity of ICAM-1, VCAM-1, and E-selectin in TNF- $\alpha$ -activated tetraspanin siRNA-transfected cells. Data represent the mean of 2 independent experiments  $\pm$ SD as the percentage of the expression referred to that of TNF- $\alpha$ -activated negative control siRNA-transfected cells. (C) Analysis of the adhesion of PBLs to tetraspanin-interfered cells under static conditions. PBLs were loaded with BCECF-AM (2',7'-bis(2-carboxyethyl)-5(6)-carboxyfluorescein acetoxymethyl ester) fluorescent probe and allowed to adhere in serum-free medium on confluent TNF- $\alpha$ -activated HUVEC monolayers for 15 minutes at 37°C. After washing, the percentage of adhesion was quantified in a fluorimeter and depicted as the mean  $\pm$ SD with respect to the adhesion levels of the negative siRNA-transfected cells in 3 different experiments performed in triplicate. (D) siRNA-transfected HUVEC monolayers were seeded onto Transwell inserts and activated with 20 ng/mL of TNF- $\alpha$  for 20 hours. Then, human peripheral blood lymphocytes were added to the upper compartment and SDF-1 $\alpha$ -containing medium (100 ng/mL) was added to the lower compartment. Cells were allowed to migrate for 2 hours and analyzed by flow cytometry. Data represent the mean  $\pm$ SD of a representative experiment performed in triplicate. \*\* $P < .005$  in a Student *t* test. (E) Tetraspanin interference augments PBL detachment under shear stress. The percentage (mean  $\pm$ SD) of remaining adherent cells is represented for the different flow rates in 4 fields of a representative experiment. ■ indicates negative siRNA; ▲, CD9 siRNA; and ×, CD151 siRNA. \* $P < .02$ ; \*\* $P < .005$  in a Student *t* test. (F) Effect of tetraspanin siRNA on lymphocyte adhesion and transmigration under flow conditions. Activated endothelium transfected with specific siRNA oligos for tetraspanins CD9 or CD151 or the negative control oligonucleotide were activated with TNF- $\alpha$ . Thereafter, PBLs were allowed to adhere and transmigrate under physiologic flow conditions (1.8 dyn/cm<sup>2</sup>) for 10 min. Quantification of rolling, adhesion, transmigration, and detachment events was performed from minute 3.5 to minute 6.5 of perfusion. Values correspond to the arithmetic mean  $\pm$ SEM of the total number of PBLs interacting with the endothelial monolayer in the 6 different fields analyzed ( $\times 20$  objective) from a representative experiment. The total number of PBLs (*n*) interacting with the HUVEC monolayer in each condition is depicted in the legend of the x-axis. \* $P < .02$  in a Student *t* test.

This cell system allowed us to assess the adhesion mediated independently by ICAM-1 or VCAM-1 in the presence or the absence of CD9. As shown in Figure 6B, binding of K562 transfectants to Colo320 cells was selective and completely dependent on the expression of ICAM-1 or VCAM-1, since no significant binding was observed with untransfected K562 cells or to untransfected Colo320 or Colo320CD9 cells (Figure 6B, and data not shown). Interestingly, VCAM-1- and ICAM-1-mediated binding was augmented by the presence of CD9 on Colo320 cells (Figure 6B). In the case of ICAM-1/LFA-1 binding, the experiments required the addition of Mn<sup>2+</sup> for LFA-1 activation on K562 cells, which resulted in a strong aggregation with Colo320 cells that partially masked the effect of CD9 (Figure 6B).

To further assess the specific contribution of CD9 in the generation of adhesion molecule/tetraspanin microdomains, we assayed the heterotypic binding of K562  $\alpha 4$  transfectants with Colo320 cells that stably express chimeric proteins made up of CD9 and CD82. All chimeric proteins were efficiently expressed at the plasma membrane (Figure 6C, flow cytometry analysis). The first chimera used coded for the N-terminal region of CD9 and the whole LEL and fourth transmembrane region belonged to CD82 (Colo320-CD9  $\times$  82) and behaved as Colo320 wild-type (wt) cells

in regard to VCAM-1-mediated binding (Figure 6C). To map the functionally relevant region of CD9, we used a second chimera with a chimeric LEL comprising the first half of CD82 LEL and the second half of CD9 LEL, where important residues for association with other transmembrane proteins reside (Colo320-CD82CCG9). This chimeric protein was able to enhance VCAM-1-mediated adhesion, even though not to the same extent as wild-type CD9. These data suggest that CD82 is not capable of replacing CD9 in the organization of endothelial-like tetraspanin-based domains in Colo320 cells and confirm that the LEL is an important functional region in CD9. Altogether, these data indicate that proper tetraspanin microdomains are necessary for the adhesive function of VCAM-1 and ICAM-1.

## Discussion

It is well established that tetraspanins interact in multiprotein domains with other transmembrane proteins.<sup>3,4,6,36</sup> Moreover, antibody crosslinking of tetraspanins usually triggers the same cellular responses as antibodies directed to their associated partners, indicating that they conform functional entities.<sup>5,36</sup> Herein, we



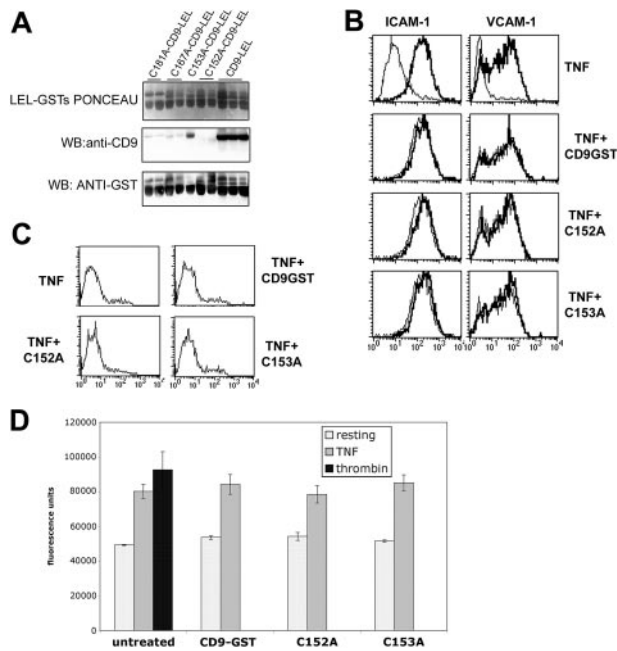


**Figure 4. Characterization of the soluble peptide CD9-LEL-GST and its mutants.** (A) LEL-GST fusion proteins of human CD9, as well as point mutations to Ala of Cys 152, 153, 167, and 181 were generated, produced in bacterial cultures, and isolated by affinity columns of Glutathione-Sepharose. Eluted purified proteins were then analyzed by Ponceau staining and Western blot against CD9 (VJ1/20 mAb) or GST. (B) Flow cytometry analysis of the expression of ICAM-1 and VCAM-1 in HUVECs preincubated with CD9-GST or its point mutants. Thin lines in the upper panels correspond to the expression of resting cells. Thin lines on the following panels correspond to cells treated with TNF- $\alpha$  alone. Thick lines correspond to the expression in cells treated for 20 hours with TNF- $\alpha$  alone (top row) or in combination with the different soluble LEL-GST peptides. (C) Propidium iodide profiles of cells treated for 20 hours with TNF- $\alpha$  alone or in combination with the different soluble LEL-GST peptides. (D) Paracellular permeability analysis of HUVEC monolayers preincubated with the different soluble LEL-GST peptides. Thrombin was added at 0.1 U/mL at the time of addition of the fluorescent dextran. Data represent the mean  $\pm$ SD of a representative experiment performed in duplicate.

describe the lateral association of ICAM-1 and VCAM-1 with tetraspanins at the contact area between leukocytes and endothelial cells. Remarkably, the function of these endothelial adhesion molecules can be directly modulated by the tetraspanin-associated moieties.

In contrast to lipid rafts, tetraspanins form a network based on protein-protein interactions, which might be modulated by differential protein expression or posttranslational modifications. In addition, tetraspanins are palmitoylated proteins that interact directly with cholesterol<sup>8-10,37</sup> and under certain conditions are also recovered in the light fractions of sucrose gradients.<sup>7</sup> Thus, tetraspanin webs or microdomains could be envisioned as a subtype of lipid rafts. In this regard, it has been suggested that the size of tetraspanin-based microdomains can be as small as lipid rafts.<sup>16</sup> Moreover, tetraspanin microdomains can be also important for intracellular signaling events, since they are able to associate with phosphatidylinositol 4-kinase (PI4-K)<sup>38</sup> and protein kinase C (PKC).<sup>39</sup> Our studies indicate that the composition of endothelial tetraspanin microdomains changes during the transmigration process. Thus, apical domains would be enriched in CD9, whereas in ventral domains CD151 is more highly represented. On the other hand, tetraspanins are also associated with integrin receptors at intercellular junctions.<sup>25,40</sup> These data suggest the existence of different tetraspanin microdomains, which might coalesce and diverge during cell activation, adhesion, or transmigration. Furthermore,

both ICAM-1 and VCAM-1 are anchored to the actin cytoskeleton through the association of ERM proteins to their cytoplasmic tails.<sup>23,24</sup> The linkage of Ig receptors to the cytoskeleton might indicate that tetraspanin microdomains are not floating freely on the plasma membrane but are connected to the cortical actin cytoskeleton.

Tetraspanins have been implicated in several cellular functions, mainly by the use of monoclonal antibodies.<sup>3-6</sup> Our results show that soluble CD9-LEL-GST peptides or tetraspanin-specific siRNA inhibit leukocyte transmigration and enhance their detachment by shear stress, supporting the functional role of tetraspanins in transendothelial migration. Similar GST fusion proteins have been reported to be inhibitory in sperm-egg fusion assays.<sup>31,41</sup> These LEL-GSTs are a valuable tool, without the effects of detergents or cholesterol-depleting agents, which affect the physical properties of the plasma membrane. The tertiary structure of these LEL proteins is very dependent on the proper disulphide bond formation. Thus, mutation of any of the 4 Cys in CD9 greatly reduces the recognition in Western blot by an anti-CD9 mAb and completely abolishes functional activity.

Endothelial tetraspanins are highly expressed and show a very slow turnover, so that partial protein knocking down by siRNA is observed only after 3 to 6 days. Although no complete abrogation of tetraspanin expression was attained, it turned out to be more than sufficient to exert a significant functional effect. Interestingly, a compensatory effect on other tetraspanin expression was observed, suggesting that a tight regulation of the overall tetraspanin load at

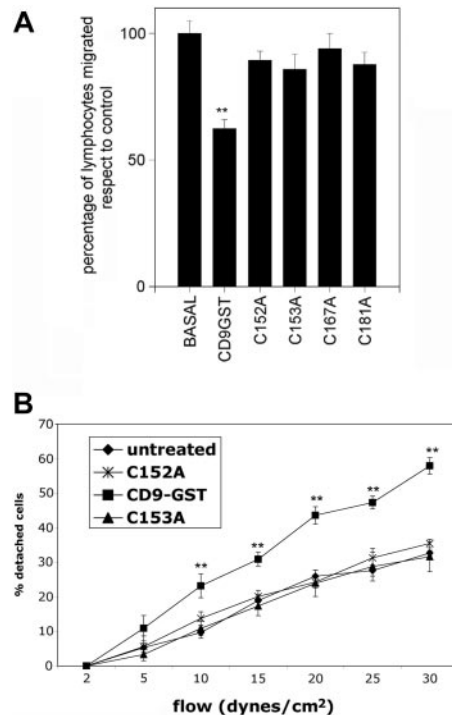


**Figure 5. CD9-LEL-GST inhibits leukocyte transendothelial migration and promotes cell detachment under flow.** (A) CD9-LEL-GST peptide inhibits transendothelial lymphoid migration in Transwells. HUVEC monolayers were activated with TNF- $\alpha$  alone or in combination with the different LEL-GST peptides. Then, human PBLs were added to the upper compartment and allowed to migrate for 5 to 7 hours. Cell migration was analyzed by flow cytometry and represented as the mean  $\pm$ SEM with respect to control untreated monolayers, of 4 independent experiments performed in duplicate. \*\* $P < .005$  in a Student  $t$  test. (B) Preincubation with CD9 LEL-GST fusion protein augments detachment under flow conditions. The percentage of detachment of PBLs was analyzed in 8 to 10 fields under increasing flow rates and represented as the mean  $\pm$ SEM.  $\blacklozenge$  indicates untreated cells;  $\times$ , C152A;  $\blacksquare$ , CD9-GST; and  $\blacktriangle$ , C153A. \*\* $P < .005$  in a Student  $t$  test.

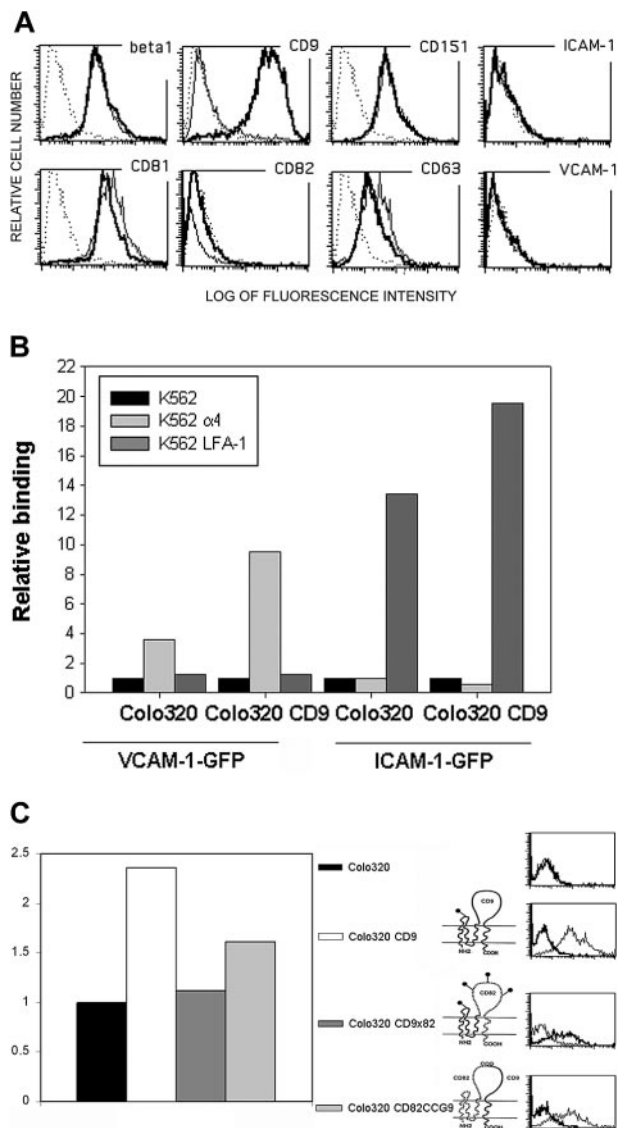


**Figure 6. Enhanced ICAM-1 and VCAM-1 adhesive function requires an appropriate tetraspanin environment.** (A) Flow cytometry analysis of the expression of  $\beta_1$  integrin (TS2/16 mAb), tetraspanins (anti-CD9 VJ1/20, anti-CD151 LIA1/1, anti-CD81 I.33.2.2, anti-CD82 TS82, and anti-CD63 TEA3/18 mAbs), ICAM-1 (HU5/3), and VCAM-1 (P8B1) in Colo320 cells (thin lines) or CD9 stably transfected Colo320 cell line (thick lines). Negative control PX63 is shown in dotted lines. (B) Heterotypic intercellular binding of K562 cell lines (parental and K562  $\alpha 4$  and K562 LFA-1 integrin transfectants) to Colo320 and Colo320CD9 cells transiently transfected with GFP-tagged versions of VCAM-1 and ICAM-1. Data are calculated as the ratio of double-positive aggregates (GFP-Colo320/CM-TMR K562) versus the nonaggregated GFP<sup>+</sup> cells. Graph depicts the relative binding referred to the aggregation obtained with parental K562 cells (that ranged from 10% to 20% of the total GFP<sup>+</sup> cells in the different transient transfections in the experiment shown) in a representative experiment out of 6 performed. (C) Heterotypic intercellular binding of K562 $\alpha 4$  integrin-stable transfectants to VCAM-1-GFP transiently transfected Colo320 cells and the different chimeric clones of CD9/CD82. Data are calculated as the ratio of double-positive aggregates (GFP-Colo320/CM-TMR K562) versus the total number of GFP<sup>+</sup> cells. Graph depicts relative binding referred to the aggregation of Colo320-VCAM-1-GFP cells in a representative experiment out of 3 (11% of the total GFP<sup>+</sup> cells in the experiment depicted). On the right, flow cytometry analysis of the expression with anti-CD9 (10B1, which also recognizes the chimeric CD9/CD82 loop; thin lines) and CD82 (TS82; thick lines) of the different chimeric clones is shown.

the plasma membrane exists. Nevertheless, as demonstrated also by the heterologous Colo320 cell system, the repertoire of tetraspanins is also crucial for the proper adhesive function of ICAM-1 and VCAM-1. Tetraspanin siRNA affected ICAM-1 and VCAM-1 expression, which suggests a possible role for tetraspanins in early

biosynthetic events. In this regard, it has been previously described that CD9 associates with the  $\beta_1$  integrin precursor prior to reaching the plasma membrane.<sup>42</sup> In a similar way, CD19 expression was selectively reduced in CD81-deficient mice, being the defect located after the endoplasmic reticulum.<sup>43</sup> However, tetraspanin interference only affected ICAM-1- and VCAM-1-mediated adhesion when assayed under stringent flow conditions. Moreover, CD9-LEL-GST peptide incubation had no effect on ICAM-1 and VCAM-1 induction but it did affect their function under shear stress. These data make both experimental approaches complementary and strongly suggest that membrane presentation into the appropriate microdomains of these receptors is functionally relevant for their proper adhesive function. Furthermore, the direct regulation of ICAM-1 and VCAM-1 adhesive function by the proper tetraspanin environment is revealed in the heterologous system of aggregation between Colo320 cells and K562 transfectants. Our data with Colo320 cells also rule out the possible involvement of a putative tetraspanin ligand on leukocytes, since their heterotypic adhesion is completely dependent on ICAM-1 or VCAM-1 expression.

The fact that ICAM-1 and VCAM-1 are included in tetraspanin-based microdomains might favor the efficient transition from the rolling step, in which VCAM-1 is involved,<sup>44,45</sup> to the firm adhesion of leukocytes via both VCAM-1 and ICAM-1 ligation,<sup>46,47</sup> to finally proceed to diapedesis. The possibility that selectins or other endothelial adhesion molecules are constituents of these endothelial tetraspanin microdomains cannot be ruled out. Another endothelial Ig adhesion molecule such as PECAM-1, also involved in transmigration,<sup>48</sup> is partially redistributed to the docking structure (not shown). In this regard, the effect of tetraspanin knocking down during the rolling and transmigration steps deserves further analysis using experimental settings specifically designed for the study of these processes. In this scenario, it could be postulated that tetraspanin microdomains would act as specialized platforms that cluster the appropriate adhesion receptors necessary for the rapid kinetics of leukocyte extravasation process.

Inclusion of ICAM-1 and VCAM-1 into tetraspanin domains is necessary for their proper function under dynamic conditions such as shear stress. This phenomenon could be explained by a possible role of tetraspanins in the preclustering or avidity regulation of endothelial adhesion receptors. Avidity regulation of the mitogenic activity of the membrane-anchored heparin-binding epidermal growth factor-like growth factor (HB-EGF) by its association with CD9 has been demonstrated.<sup>49,50</sup> Recent observations show that tetraspanin networks are able to cluster class II major histocompatibility complex (MHC) molecules bearing restricted repertoires of peptides,<sup>16</sup> thus facilitating antigen peptide presentation. Furthermore, CD81 also regulates very late antigen (VLA)-4- and VLA-5-mediated adhesion by enhancing integrin avidity independently of ligand binding.<sup>51</sup> This phenomenon also facilitated leukocyte firm adhesion by strengthening VLA-4-VCAM-1 interaction acting on the leukocyte side.

The inclusion of adhesion receptors into tetraspanin domains could also affect their conformation, up-regulating their binding to integrins. In this regard, we have recently described a monoclonal antibody that preferentially recognizes CD9 when associated with  $\alpha_6\beta_1$  integrin.<sup>26</sup> The possibility of reciprocal conformational changes in tetraspanin-associated proteins cannot be excluded. In this regard, CDw78 mAbs recognize human leukocyte antigen (HLA)-DR only when included into tetraspanin domains,<sup>52</sup> although the possibility of a conformational change in HLA-DR



because of its interaction with tetraspanins has not been determined. Lately, CD151 knock-out mice show a mild deficiency in outside-in activation of  $\alpha_{IIb}\beta_{III}$  integrin in platelets,<sup>53</sup> whereas human CD151 deficiency causes a more aggressive phenotype with renal, skin, hearing, and erythropoiesis defects<sup>54</sup>. Thus, several lines of evidence support a functional role for tetraspanin-based microdomains in different cellular functions. In this report we demonstrate by different complementary experimental approaches, both on primary cells and assessing endogenous proteins, and in an heterologous system, that the adhesive function of ICAM-1 and VCAM-1 is directly modulated by their inclusion in a microdomain containing the appropriate repertoire of tetraspanins. This effect

was shown to be crucial in an important physiologic process such as leukocyte extravasation and may have a great relevance not only in homing and inflammation but also in haematopoietic developmental stages at the bone marrow.<sup>55-57</sup>

## Acknowledgments

We thank E. Rubinstein for the original chimeric constructs of CD9/CD82 and the 10B1 mAb, and R. Gonzalez-Amaro for critical reading of the manuscript.

## References

1. Simons K, Toomre D. Lipid rafts and signal transduction. *Nat Rev Mol Cell Biol*. 2000;1:31-41.
2. Pike LJ. Lipid rafts: bringing order to chaos. *J Lipid Res*. 2003;44:655-667.
3. Berditchevski F. Complexes of tetraspanins with integrins: more than meets the eye. *J Cell Sci*. 2001;114:4143-4151.
4. Boucheix C, Rubinstein E. Tetraspanins. *Cell Mol Life Sci*. 2001;58:1189-1205.
5. Hemler ME. Specific tetraspanin functions. *J Cell Biol*. 2001;276:1103-1107.
6. Yáñez-Mó M, Mittelbrunn M, Sánchez-Madrid F. Tetraspanins and intercellular interactions. *Microcirculation*. 2001;8:153-168.
7. Claas C, Stipp CS, Hemler ME. Evaluation of prototype TM4SF protein complexes and their relation to lipid rafts. *J Biol Chem*. 2001;276:7974-7984.
8. Charrin S, Manie S, Oualid M, Billard M, Boucheix C, Rubinstein E. Differential stability of tetraspanin/tetraspanin interactions: role of palmitoylation. *FEBS Lett*. 2002;516:139-144.
9. Yang X, Claas C, Kraeft SK, et al. Palmitoylation of tetraspanin proteins: modulation of CD151 lateral interactions, subcellular distribution, and integrin-dependent cell morphology. *Mol Biol Cell*. 2002;13:767-781.
10. Berditchevski F, Odintsova E, Sawada S, Gilbert E. Expression of the palmitoylation-deficient CD151 weakens the association of alpha 3 beta 1 integrin with the tetraspanin-enriched microdomains and affects integrin-dependent signaling. *J Biol Chem*. 2002;277:36991-37000.
11. Stipp C, Kolesnikova T, Hemler M. Functional domains in tetraspanin proteins. *Trends Biochem Sci*. 2003;28:106-112.
12. Deng J, Dekruyff RH, Freeman GJ, Umetsu DT, Levy S. Critical role of CD81 in cognate T-B cell interactions leading to Th2 responses. *Int Immunol*. 2002;14:513-523.
13. Chen MS, Tung KS, Coonrod SA, et al. Role of the integrin-associated protein CD9 in binding between sperm ADAM 2 and the egg integrin alpha6beta1: implications for murine fertilization. *Proc Natl Acad Sci U S A*. 1999;96:11830-11835.
14. Mittelbrunn M, Yáñez-Mó M, Sancho D, Urza A, Sánchez-Madrid F. Cutting edge: dynamic redistribution of tetraspanin CD81 at the central zone of the immune synapse in both T lymphocytes and APC. *J Immunol*. 2002;169:6691-6695.
15. Knobloch K, Wright M, Ochslein A, et al. Targeted inactivation of the tetraspanin CD37 impairs T-cell-dependent B-cell response under suboptimal costimulatory conditions. *Mol Cell Biol*. 2000;20:5363-5369.
16. Kropshofer H, Spindeldreher S, Rohn TA, et al. Tetraspan microdomains distinct from lipid rafts enrich select peptide-MHC class II complexes. *Nat Immunol*. 2002;3:61-68.
17. Kaji K, Oda S, Shikano T, et al. The gamete fusion process is defective in eggs of CD9-deficient mice. *Nat Genet*. 2000;24:279-282.
18. Le Naour F, Rubinstein E, Jasmin C, Prenant M, Boucheix C. Severely reduced female fertility in CD9-deficient mice. *Science*. 2000;287:319-321.
19. Miller BJ, Georges-Labouesse E, Primakoff P, Myles DG. Normal fertilization occurs with eggs lacking the integrin alpha6beta1 and is CD9-dependent. *J Cell Biol*. 2000;149:1289-1296.
20. Miyado K, Yamada G, Yamada S, et al. Requirement of CD9 on the egg plasma membrane for fertilization. *Science*. 2000;287:321-324.
21. von Andrian U, Hasslen S, Nelson R, Erlandsen S, Butcher E. A central role for microvillous receptor presentation in leukocyte adhesion under flow. *Cell*. 1995;82:989-999.
22. Barreiro O, Vicente-Manzanares M, Urzainqui A, Yáñez-Mó M, Sánchez-Madrid F. Interactive protrusive structures during leukocyte adhesion and transendothelial migration. *Front Biosci*. 2004;9:1843-1863.
23. Barreiro O, Yáñez-Mó M, Serrador JM, et al. Dynamic interaction of VCAM-1 and ICAM-1 with moesin and ezrin in a novel endothelial docking structure for adherent leukocytes. *J Cell Biol*. 2002;157:1233-1245.
24. Heiska L, Alfthan K, Gronholm M, Vilja P, Vaheri A, Carpen O. Association of ezrin with intercellular adhesion molecule-1 and -2 (ICAM-1 and ICAM-2): regulation by phosphatidylinositol 4, 5-bisphosphate. *J Biol Chem*. 1998;273:21893-21900.
25. Yáñez-Mó M, Alfranca A, Cabañas C, et al. Regulation of endothelial cell motility by complexes of tetraspan molecules CD81/TAPA-1 and CD151/PETA-3 with alpha3beta1 integrin localized at endothelial lateral junctions. *J Cell Biol*. 1998;141:791-804.
26. Gutierrez-Lopez MD, Ovalle S, Yáñez-Mó M, et al. A functionally relevant conformational epitope on the CD9 tetraspanin depends on the association with activated beta-1 integrin. *J Biol Chem*. 2003;278:208-218.
27. Serrador JM, Alonso-Lebrero JL, del Pozo MA, et al. Moesin interacts with the cytoplasmic region of intercellular adhesion molecule-3 and is redistributed to the uropod of T lymphocytes during cell polarization. *J Cell Biol*. 1997;138:1409-1423.
28. Montoya M, Holtmann K, Snapp K, et al. Memory B lymphocytes from secondary lymphoid organs interact with E-selectin through a novel glycoprotein ligand. *J Clin Invest*. 1999;103:1317-1327.
29. Peñas PF, García-Diez A, Sánchez-Madrid F, Yáñez-Mó M. Tetraspanins are localized at motility-related structures and involved in normal human keratinocyte wound healing migration. *J Invest Dermatol*. 2000;114:1126-1135.
30. Longo N, Yáñez-Mó M, Mittelbrunn M, et al. Regulatory role of tetraspanin CD9 in tumor-endothelial cell interaction during transendothelial invasion of melanoma cells. *Blood*. 2001;98:3717-3726.
31. Higginbottom A, Takahashi Y, Bolling L, et al. Structural requirements for the inhibitory action of the CD9 large extracellular domain in sperm/ooocyte binding and fusion. *Biochem Biophys Res Commun*. 2003;311:208-214.
32. Dominguez-Jimenez C, Yáñez-Mó M, Carreira A, et al. Involvement of alpha3 integrin/tetraspanin complexes in the angiogenic response induced by angiotensin II. *FASEB J*. 2001;15:1457-1459.
33. Lusinskas FW, Kansas GS, Ding H, et al. Monocyte rolling, arrest and spreading on IL-4 activated vascular endothelium under flow is mediated via sequential action of L-selectin, beta-1-integrins, and beta-2-integrins. *J Cell Biol*. 1994;125:1417-1427.
34. Sincock PM, Fitter S, Parton RG, Berndt MC, Gamble JR, Ashman LK. PETA-3/CD151, a member of the transmembrane 4 superfamily, is localized to the plasma membrane and endocytic system of endothelial cells, associates with multiple integrins and modulates cell function. *J Cell Sci*. 1999;112:833-844.
35. Serru V, Le Naour F, Billard M, et al. Selective tetraspan-integrin complexes (CD81/alpha4beta1, CD151/alpha3beta1, CD151/alpha6beta1) under conditions disrupting tetraspan interactions. *Biochem J*. 1999;340:103-111.
36. Hemler ME. Integrin associated proteins. *Curr Opin Cell Biol*. 1998;10:578-585.
37. Charrin S, Manie S, Thiele C, et al. A physical and functional link between cholesterol and tetraspanins. *Eur J Immunol*. 2003;33:2479-2489.
38. Berditchevski F, Toliás KF, Wong K, Carpenter CL, Hemler ME. A novel link between integrins, transmembrane-4 superfamily proteins (CD63 and CD81), and phosphatidylinositol 4-kinase. *J Biol Chem*. 1997;272:2595-2598.
39. Zhang X, Bontrager A, Hemler M. Transmembrane-4 superfamily proteins associate with activated protein kinase C (PKC) and link PKC to specific beta(1) integrins. *J Biol Chem*. 2001;276:25005-25013.
40. Chattopadhyay N, Wang Z, Ashman LK, Brady-Kalnay SM, Kreidberg J. alpha3beta1 integrin-CD151, a component of the cadherin-catenin complex, regulated PTPase expression and cell-cell adhesion. *J Cell Biol*. 2003;163:1351-1362.
41. Zhu G, Miller B, Boucheix C, et al. Residues SFQ (173-175) in the large extracellular loop of CD9 are required for gamete fusion. *Development*. 2002;129:1995-2002.
42. Rubinstein E, Poindessous-Jazat V, Le Naour F, Billard M, Boucheix C. CD9, but not other tetraspans, associates with the beta1 integrin precursor. *Eur J Immunol*. 1997;27:1919-1927.
43. Shoham T, Rajapaksa R, Boucheix C, et al. The tetraspanin CD81 regulates the expression of CD19 during B cell development in a postendoplasmic reticulum compartment. *J Immunol*. 2003;171:4062-4072.
44. Berlin C, Bargatze R, Campbell J, et al. Alpha 4 integrins mediate lymphocyte attachment and

- rolling under physiologic flow. *Cell*. 1995;80:413-422.
45. Alon R, Kassner P, Carr M, Finger E, Hemler M, Springer T. The integrin VLA-4 supports tethering and rolling in flow on VCAM-1. *J Cell Biol*. 1995;128:1243-1253.
  46. Butcher EC. Leukocyte-endothelial cell recognition: three (or more) steps to specificity and diversity. *Cell*. 1991;67:1033-1036.
  47. Springer TA. Traffic signals for lymphocyte recirculation and leukocyte emigration: the multistep paradigm. *Cell*. 1994;76:301-314.
  48. Muller WA, Weigl SA, Deng X, Phillips DM. PECAM-1 is required for transendothelial migration of leukocytes. *J Exp Med*. 1993;178:449-460.
  49. Higashiyama S, Iwamoto R, Goishi K, et al. The membrane protein CD9/DRAP 27 potentiates the juxtacrine growth factor activity of the membrane-anchored heparin-binding EGF-like growth factor. *J Cell Biol*. 1995;128:929-938.
  50. Nakamura K, Mitamura T, Takahashi T, Kobayashi T, Mekada E. Importance of the major extracellular domain of CD9 and the epidermal growth factor (EGF)-like domain of heparin-binding EGF-like growth factor for up-regulation of binding and activity. *J Biol Chem*. 2000;275:18284-18290.
  51. Feigelson S, Grabovsky V, Shamri R, Levy S, Alon R. The CD81 tetraspanin facilitates instantaneous leukocyte adhesion strengthening to vascular cell adhesion molecule 1 (VCAM-1) under shear flow. *J Biol Chem*. 2003;278:51203-51212.
  52. Drbal K, Angelisova P, Rasmussen A, Hilgert I, Funderud S, Horejsi V. The nature of the subset of MHC class II molecules carrying the CDw78 epitopes. *Int Immunol*. 1999;11:491-498.
  53. Lau LM, Wee JL, Wright MD, et al. The tetraspanin superfamily member, CD151 regulates outside-in integrin  $\alpha$ IIb $\beta$ 3 signalling and platelet function. *Blood*. 2004;104:2368-2375.
  54. Karamatic Crew V, Burton N, Kagan A, et al. CD151, the first member of the tetraspanin (TM4) superfamily detected on erythrocytes, is essential for the correct assembly of human basement membranes in kidney and skin. *Blood*. 2004;108:2217-2223.
  55. Leuker CE, Labow M, Müller W, Wagner N. Neonatally induced inactivation of the vascular cell adhesion molecule 1 gene impairs B cell localization and T cell-dependent humoral immune response. *J Exp Med*. 2001;193:755-767.
  56. Koni PA, Joshi SK, Temann UA, Olson D, Burkly L, Flavell RA. Conditional vascular cell adhesion molecule 1 deletion in mice: impaired lymphocyte migration to bone marrow. *J Exp Med*. 2001;193:741-753.
  57. Dittel BN, LeBien TW. Reduced expression of vascular cell adhesion molecule-1 on bone marrow stromal cells isolated from marrow transplant recipients correlates with a reduced capacity to support human B lymphopoiesis in vitro. *Blood*. 1995;86:2833-2841.



**blood**<sup>®</sup>

2005 105: 2852-2861  
doi:10.1182/blood-2004-09-3606 originally published online  
December 9, 2004

## **Endothelial tetraspanin microdomains regulate leukocyte firm adhesion during extravasation**

Olga Barreiro, María Yáñez-Mó, Mónica Sala-Valdés, María Dolores Gutiérrez-López, Susana Ovalle, Adrian Higginbottom, Peter N. Monk, Carlos Cabañas and Francisco Sánchez-Madrid

---

Updated information and services can be found at:  
<http://www.bloodjournal.org/content/105/7/2852.full.html>

Articles on similar topics can be found in the following Blood collections  
[Cell Adhesion and Motility](#) (790 articles)  
[Immunobiology](#) (5467 articles)

---

Information about reproducing this article in parts or in its entirety may be found online at:  
[http://www.bloodjournal.org/site/misc/rights.xhtml#repub\\_requests](http://www.bloodjournal.org/site/misc/rights.xhtml#repub_requests)

Information about ordering reprints may be found online at:  
<http://www.bloodjournal.org/site/misc/rights.xhtml#reprints>

Information about subscriptions and ASH membership may be found online at:  
<http://www.bloodjournal.org/site/subscriptions/index.xhtml>